Magnetic/Ceramic Multi-material processed by LPBF additive manufacturing

M.A. Amitouche [1,2], O. Marconot [1], Y. Danlos [1], A. Ospina [2], N. Fenineche [1]

1.ICB PMDM LERMPS, UMR 6303, CNRS, Université Marie et Louis Pasteur, UTBM, Belfort, France.

2. Roberval, UMR 7337, CNRS, Université de Technologie de Compiègne, Compiègne, France

Abstract: Electric motors are composed of laminated sheets of FeSi3, separated by insulating polymer layers. The ferromagnetic material FeSi6.5 has lower magnetic losses than FeSi3, making it a promising candidate for the manufacture of electric motors. However, its high silicon content complicates its production by conventional lamination processes. Additive manufacturing offers a viable alternative, but it is currently limited to single-material structures. Research on multi-material additive manufacturing is still in its early stages. The challenge is to manufacture laminated electric motors using additive manufacturing with thin ceramic insulating layers and FeSi6.5 layers. We have developed a system to modify our LPBF machine for bi-material processes and to optimize the ceramic/metal interface.

Keywords: Magnetic material, Additive Manufacturing, bi-material, multi-material

1. INTRODUCTION

Electric machines (EM) are essential in modern industry for various applications, from propulsion to electricity generation. Additive manufacturing offers a promising alternative for producing soft magnetic materials, thereby reducing energy losses.[1] [2].

Additive manufacturing of ferromagnetic materials, particularly FeSi, FeNi, and FeCo alloys, aims to enhance their mechanical and magnetic properties. FeSi alloys are the most commonly used due to their low coercivity (Hc = [50–100 A/m]), high magnetic flux density (Bs = [1.6–1.8 T]), and significant relative permeability (μr = [10,000–12,000]). [3] [4] The FeSi alloy with 6.5% silicon stands out for its high electrical resistivity, zero magnetostriction, and low magnetocrystalline anisotropy, making it ideal for magnetic devices.[3] [4] [5]. High-silicon steels are brittle. Additive manufacturing offers flexibility and improved magnetic performance, and also enables the creation of complex composite materials, improving the properties of electrical steels. While FeSi6.5 demonstrates optimal magnetic performance, eddy current losses continue to pose a challenge. [2] [4] [6] [7] [8]

Electric motors are composed of thin layers of FeSi3 alternating with insulating polymer layers. In additive manufacturing, we aim to replace the polymer with ceramics and FeSi3 with FeSi6.5. However, ceramics and metals have very different properties, particularly in terms of melting point. To address this issue, we have chosen to use yttria-stabilized zirconia (ZrO_2-Y_2O_3), a ceramic whose coefficient of thermal expansion is very close to that of steel. [9] [10] [11]

In this study, we have modified our laser powder bed fusion (LPBF) system, originally designed for single-material fabrication in a monolithic block, to enable the production of laminated materials. The primary objective is to alternate layers of ceramic and ferromagnetic FeSi6.5. Initially, we characterized the powders used for both materials, FeSi6.5 and ZrO_2-Y_2O_3, defining their essential properties to ensure optimal compatibility with the LPBF process. Subsequently, we detailed the modifications implemented to facilitate multi-material fabrication. In the second phase, we exhibhit optimization of the processing parameters for each material individually to establish suitable manufacturing conditions. Following this, we develop the deposition protocol for ZrO_2-Y_2O_3 ceramic onto ferromagnetic FeSi6.5, considering the thermal and physicochemical interactions between the two materials. Finally, in the results section, we present the fabrication outcomes for each material independently, followed by the results of the laminated composite structure. The study concludes with a comprehensive analysis of the findings, addressing the challenges encountered and the advancements achieved in the process

2. MATERIALS AND METHODS

2.1. Powder characterization:

The manufacturing of FeSi6.5% materials varies depending on the machines due to differences in machine characteristics. The FeSi6.5 powder was dried to improve its adhesion and flowability, with a particle size distribution of 15 to 45 μm, and particles larger than 63 μm were reduced by sieving. The raw material for the insulation is a 7% ZrO_2-Y_2O_3 powder, also sieved to reduce particles larger than 63 μm, with a particle size distribution of 15 to 45 μm.

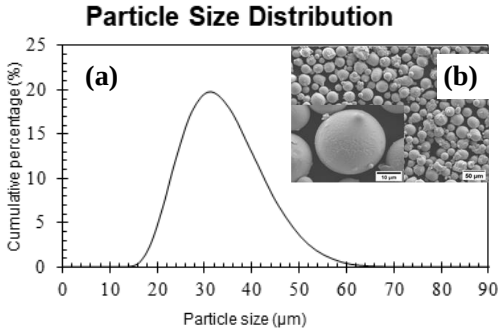

Fig. 1.(a) Particle size distribution and (b) scanning electron microscopy (SEM) view morphology of Fe6.5%wtSi powder after sieving at 63μm mesh

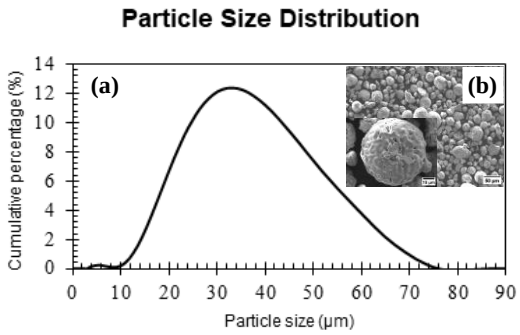

Fig. 2.(a) Particle size distribution and (b) scanning electron microscopy (SEM) view morphology of YSZ powder after sieving at 63µm mesh

2.2. *Manufacturing process:*

The experiments were carried out in a specific selective laser melting machine at the ICB-PMDM laboratory, A Realizer SLM250 machine. An Ytterbium fiber laser source with a maximum theoretical power output of 120 W and a wavelength of 1064 µm was used. The laser focus beam has a diameter of 34 µm. The building chamber dimension is 250 × 250 × 250 mm. The machine was filled with a shielding gas during all experiments to remove smoke and maintain a stable pressure. The chamber was purged of residual oxygen below 0.1% to avoid oxidation. The laser scanning mode was continuous. However, the laser displacement was driven by two mirrors fixed on a stepper motor to insure X and Y directions, with a galvanometric head. A continuous weld bead was formed point by point, with a distance Pdist between each point. The laser remained at each point for an exposure time of Texpo and then moves to the next point at the Pdist distance along the trajectory. Thus, Pdist and Texpo determine the effective scanning speed Fig.4.

The system developed for integration into the LPBF machine consists of a powder distributor with two separate powder feeders, allowing the manufacturing machine to be fed with one or two powders Fig.3a. This distributor operates with argon gas, which pushes the powder through a pipe into the build chamber. This system allows switching from one powder to another or simultaneous feeding with both. For spreading powder on the build bed, two powder inlet chambers are integrated into the coater. These two chambers are separate, and each chamber contains different materials.

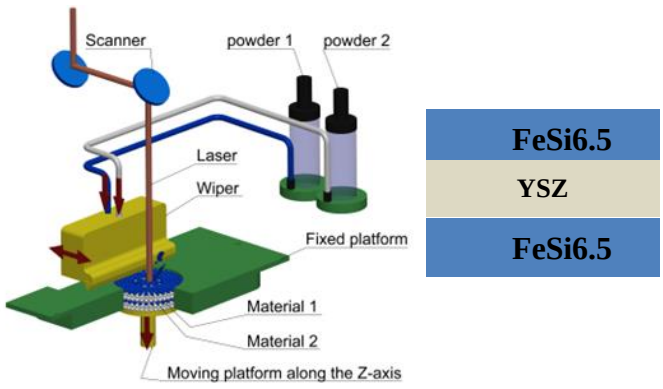

Fig. 3. Schematic representation of the multi-material powder feed system for the laser powder bed fusion machine

2.3. *Experimental*

In this section, we systematically varied the process parameters for both FeSi6.5 and YSZ materials to optimize fabrication conditions. Cubic metallurgical samples, measuring 8 mm × 8 mm × 4 mm for FeSi6.5 and 8 mm × 8 mm × 2 mm for YSZ ceramics, were prepared. Three sets of experiments were conducted to enhance the density of FeSi6.5 and eliminate cracks. Optimal parameters were determined by adjusting laser power, speed, and hatch distance. For the YSZ material, a constant layer thickness of 30 µm was maintained. Three experimental campaigns were carried out, and optimal parameters were identified. To explore multi-material manufacturing, we sought to create a layered structure of FeSi6.5-ceramic-FeSi6.5, prioritizing ceramic layer adhesion. Fifteen FeSi6.5 samples were deposited onto a stainless steel substrate. Subsequently, YSZ ceramic was added to these samples. To enhance adhesion, we varied the number of laser passes for one layer (1-3) and the number of ceramic layers (1-5), while alternating the laser orientation angle by 90 degrees between each layer. The primary objective of this study was to assess the influence of these parameters on adhesion quality and the overall morphology of the deposited layers.

Matériel	**FeSi6.5**	**ZrO_2-Y_2O_3 7%**
Layer thickness, t (µm)	30	30
Hatch distance, h (µm)	30	30
Laser power, P (W)	83, 88, 95	13, 18, 23, 27, 33
Scan speed, v (mm/s)	410	28 - 121
volume energy density j/mm³	224-257	303,353,403,453,503
Substrate	Inox	Inox
Plate temperature	240	240
Atmosphere	Argon	Argon

Table.1. Operational Parameters of Test Campaigns for Additive Manufacturing of FeSi6.5 and ZrO_2-Y_2O_3 Materials by LPBF

3. RESULTS AND DISCUSSION:

3.1. *Monomaterial additive manufacturing results:*

For the fabrication results of FeSi6.5, the bulk density was measured using Archimedes' principle on samples taken directly from the fabrication platform. After cutting and polishing, surface densities were analyzed using an optical microscope. During the third test campaign, the sample with the highest density was selected under the following conditions: **a constant velocity of 0.41 m/s, a fixed laser scan spacing of 30 µm, a laser spot spacing of 30 µm, and a power of 95 W**. The apparent surface density, estimated by electron microscopy, was 98.93%, while Archimedes' method yielded an internal density of 97.09%. Fig.4, Fig.5a.

The results of the two test campaigns conducted for ZrO_2-Y_2O_3 ceramic show that, during the first series of experiments, the fabrication process was stopped as soon as a completely burned but unfused powder was observed. We found that all the samples subjected to a power of 33 W were the only ones to exhibit partial fusion. Analyzing the results for the five tested

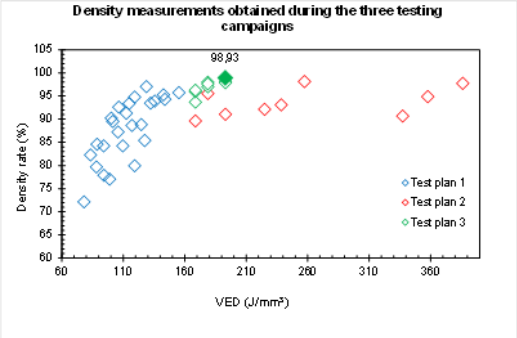

Fig. 4. Evolution of density values as a function of VED over the course of the three test plans.

energy levels, ranging from 133 to 253 J/mm³, we observed that low energy levels led to incomplete melting, while increasing the energy promoted fusion. This phenomenon can be explained by the refractory nature of our material to Laser radiation. Indeed, its low thermal conductivity limits its ability to quickly absorb a large amount of energy. However, by using 30 µm layers, the energy can be better distributed, thereby facilitating fusion. Our objective is thus to provide enough energy to reach the high melting point of this material while avoiding local overheating caused by excessive power. Consequently, we designed a new series of experiments by reducing the power and increasing the fabrication energy. In our second test campaign, we observed that power levels of 13 and 18 W were insufficient to melt the powder, regardless of the tested energy levels. In contrast, for power levels of 23, 28, and 33 W, successful melting was achieved, enabling the fabrication of samples at all energy levels. These results allowed us to identify the optimal parameters for achieving the highest density. However, the samples fabricated under these optimal conditions did not exhibit good adhesion to the stainless-steel substrate.

The parameters determined for ceramic processing in the remainder of the study are as follows: a relatively low laser power of 33 W, a scanning speed of 72 mm/s, a laser track spacing of 30 µm, and a layer thickness of 30 µm, corresponding to an energy density of 503 J/mm³. Fig.5.b.

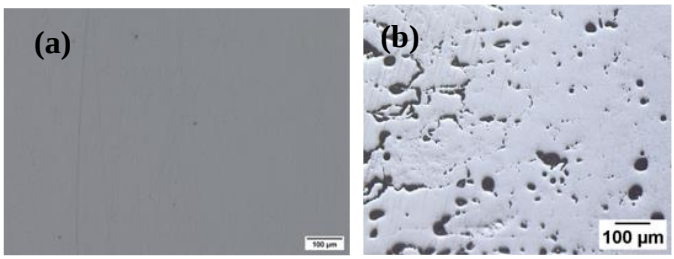

Fig. 5. Electron Microscopy of a Sample: (a) FeSi6.5 and (b) ZrO_2-Y_2O_3

3.2. *Multi-material additive manufacturing results*:

During the fabrication of YSZ ceramics on stainless steel substrates, poor adhesion of the ceramic to the metallic substrate was observed. The same phenomenon was also observed during deposition on FeSi6.5 samples.

The successive deposition of YSZ on FeSi6.5 revealed a significant presence of YSZ ceramic on the FeSi6.5 samples. The formation of this deposit was found to be directly correlated with the number of remelting performed on each layer. Indeed, the higher the number of remelting, the more homogeneous and continuous the ceramic deposit observed across the entire sample Fig.6.b.

Electron microscopy reveals the formation of an intermediate zone between FeSi6.5 and YSZ. Electron microscopy analysis shows that this zone is composed of Zr, Fe, and Si. This can be explained by the fact that during the fusion of YSZ, the melt pool depth exceeds the thickness of the YSZ layer and reaches the underlying FeSi6.5. As a result, the melt pool consists of a mixture of FeSi6.5 and YSZ. During solidification, the YSZ remains trapped within the FeSi6.5, forming this mixing zone. This zone corresponds to the diffusion of YSZ into FeSi6.5. The elemental composition of this zone varies depending on the number of remelting of the YSZ deposited layer Fig.6.a, Fig.6.b.

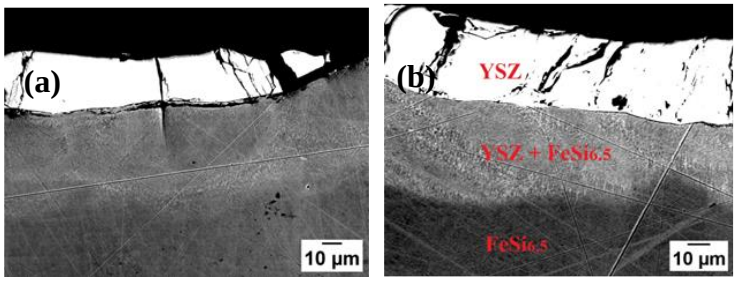

Fig. 6. These images depict samples consisting of five layers of ZrO_2-Y_2O_3 ceramic deposited on FeSi6.5.(a) Corresponds to the sample that underwent a single fusion for each ceramic layer. (b) Corresponds to the sample that underwent three fusions for each cera

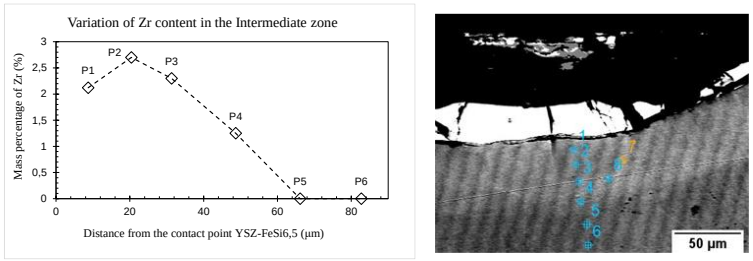

Fig. 7. The image illustrates the percentage of zirconium measured at different points in the intermediate zone.

It is observed that, for a single fusion of YSZ on FeSi6.5, Fig 7, the Zr element is more concentrated in the contrast areas of the melt pool than in the core Fig.7. Moreover, the distribution of Zr is not homogeneous. However, as the number of layer remelting increases, the distribution of Zr elements within the zone becomes more uniform.

The thickness of the intermediate zone is approximately 50 µm across all samples, regardless of the number of remeltings of the Zr layer.

3.3. Magnetic Analysis:

Fig. 8. Hysteresis Loops at 1 Hz Before and After Heat Treatment for Fe-6.5%Si Alloy Toroids Fabricated by LPBF shows two hysteresis loops measured at a frequency of 1 Hz on toroidal samples made from Fe-6.5%Si alloy using LPBF additive manufacturing.

The orange loop corresponds to the state before heat treatment, while the blue loop represents the state after heat treatment. After the heat treatment, the hysteresis loop remains similar to the one

observed before treatment at 1 Hz, indicating that the coercivity has not changed significantly. However, the post-treatment loop reaches a higher level of magnetic saturation, which can be attributed to an improvement in the material's effective magnetic density. It is also noticeable that the rise of the hysteresis loop after heat treatment is steeper than before, meaning that magnetization increases more rapidly under a low applied magnetic field. This reflects an increase in initial permeability, which is a typical feature of soft magnetic materials.

Finally, the area of the hysteresis loop which represents energy loss per cycle is visibly smaller after heat treatment, consistent with reduced magnetic losses at low frequency.

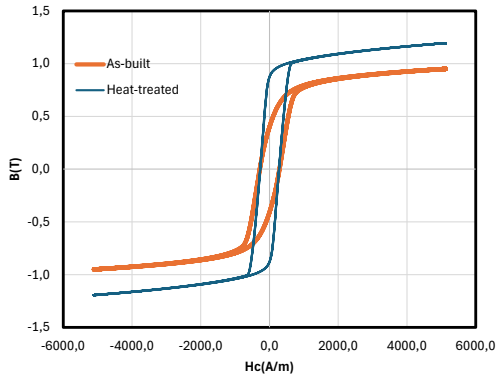

Fig. 8. Hysteresis Loops at 1 Hz Before and After Heat Treatment for Fe-6.5%Si Alloy Toroids Fabricated by LPBF

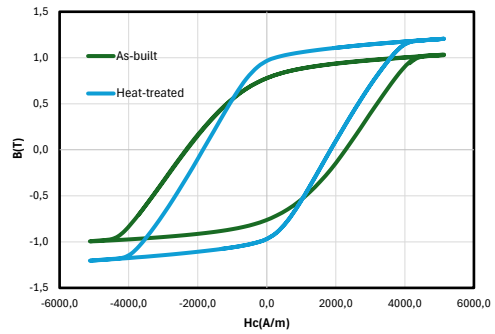

Fig. 9. Hysteresis Loops at 50 Hz Before and After Heat Treatment for Fe-6.5%Si Alloy Toroids Fabricated by LPBF

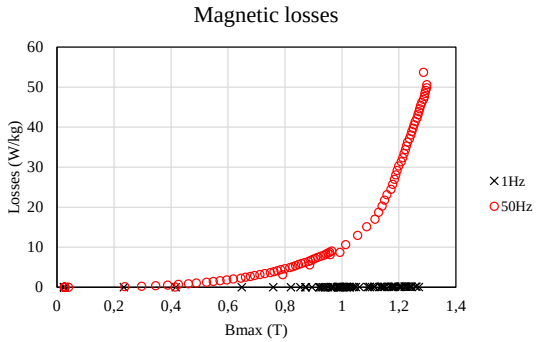

Fig. 10. Magnetic losses (W/kg) as a function of maximum magnetic induction Bmax after heat treatment at 1150 °C, comparison between 1 Hz and 50 Hz

Fig. 9. Hysteresis Loops at 50 Hz Before and After Heat Treatment for Fe-6.5%Si Alloy Toroids Fabricated by LPBF
Fig. 10. Magnetic losses (W/kg) as a function of maximum magnetic induction Bmax after heat treatment at 1150 °C, comparison between 1 Hz and 50 Hzshows the magnetic losses (W/kg) as a function of the maximum magnetic induction Bmax after heat treatment at 1150 °C. Two frequencies are compared: 1 Hz and 50 Hz.

At 1 Hz, the losses are very low since hysteresis losses dominate at this very low frequency.

At 50 Hz, the losses increase significantly, showing typical behavior for soft magnetic materials, where both hysteresis and eddy current losses contribute to the total losses.

An increase in losses is observed starting around Bmax ≈ 1.0 T, reaching over 50 W/kg at 1.3 T, indicating a strong sensitivity to losses at high frequency.

The heat treatment was effective in reducing losses at low frequency 1 Hz. However, at 50 Hz, losses remain significant at high magnetic induction, which is related to the thickness of the material layers formed during additive manufacturing, potentially promoting eddy currents. The most significant losses are primarily due to these eddy currents. Lamination helps to mitigate this phenomenon. Once lamination is completed, our goal is to reduce the total losses at 50 Hz to below 1 W/kg for a magnetic induction of 1 T.

4. Conclusions

In this study, we optimized the manufacturing parameters of FeSi6.5 and ZrO_2-Y_2O_3 materials within the framework of additive manufacturing by laser powder bed fusion (LPBF). The objective was to assess the feasibility of bi-material fabrication by defining the appropriate parameters for efficient and controlled production.

A feasibility test was conducted to deposit ceramic (ZrO_2-Y_2O_3) on a FeSi6.5 substrate. A series of experiments was carried out to validate the ceramic deposition on FeSi6.5. The results obtained were satisfactory, paving the way for future work aimed at fabricating a layered structure of the FeSi6.5-ZrO_2-Y_2O_3-FeSi6.5 type.

The results show good adhesion of the ZrO_2-Y_2O_3 ceramic after several laser passes over the deposited powder layer. The adhesion of the ceramic layer is directly dependent on the laser parameters used. Additionally, an intermediate zone was formed between the ceramic and the FeSi6.5. This zone mainly contains FeSi6.5, along with significant traces of Zr and Y, confirming the diffusion of elements.

The thickness of the intermediate zone remains constant under the tested experimental conditions. Moreover, the hardness measured in this area is higher than that of FeSi6.5 alone, highlighting the potential of this transition zone to enhance the properties of the final material.

These promising results provide a solid foundation for continuing the development of multilayer bi-material structures for advanced applications.

Acknowledgements:

The authors acknowledge the ANR – FRANCE (French National Research Agency) for its financial support of the FALSTAFF project N° ANR-22-CE08-0029-04

Declaration of Conflicts Interest:

The authors declare that they have no competing financial interests.

There are no competing interests related to this work.

There are no known conflicts of interest associated with this publication.

[1] S. Gao *et al.*, « Magnetic and mechanical properties of additive manufactured Fe-3wt.%Si material », *Journal of Magnetism and Magnetic Materials*, vol. 580, p. 170907, août 2023, doi: 10.1016/j.jmmm.2023.170907.

[2] D. Goll *et al.*, « Additive manufacturing of soft magnetic materials and components », *Additive Manufacturing*, vol. 27, p. 428-439, mai 2019, doi: 10.1016/j.addma.2019.02.021.

[3] G. Ouyang, X. Chen, Y. Liang, C. Macziewski, et J. Cui, « Review of Fe-6.5 wt%Si high silicon steel—A promising soft magnetic material for sub-kHz application », *Journal of Magnetism and Magnetic Materials*, vol. 481, p. 234-250, juill. 2019, doi: 10.1016/j.jmmm.2019.02.089.

[4] M. Zaied, A. Ospina-Vargas, N. Buiron, J. Favergeon, et N.-E. Fenineche, « Additive Manufacturing of Soft Ferromagnetic Fe 6.5%Si Annular Cores: Process Parameters, Microstructure, and Magnetic Properties », *IEEE Transactions on Magnetics*, vol. 58, nº 11, p. 1-9, nov. 2022, doi: 10.1109/TMAG.2022.3202631.

[5] A. A. V. Salazar *et al.*, « Density Analysis Based on Normalized Process Diagrams : A Comparative Review of Ferromagnetic Alloys Produced by Laser Powder Bed Fusion », in *2024 International Conference on Electrical Machines (ICEM)*, sept. 2024, p. 1-6. doi: 10.1109/ICEM60801.2024.10700463.

[6] M. Garibaldi, I. Ashcroft, J. N. Lemke, M. Simonelli, et R. Hague, « Effect of annealing on the microstructure and magnetic properties of soft magnetic Fe-Si produced via laser additive manufacturing », *Scripta Materialia*, vol. 142, p. 121-125, janv. 2018, doi: 10.1016/j.scriptamat.2017.08.042.

[7] J. Koopmann, J. Voigt, et T. Niendorf, « Additive Manufacturing of a Steel–Ceramic Multi-Material by Selective Laser Melting », *Metall Mater Trans B*, vol. 50, nº 2, p. 1042-1051, avr. 2019, doi: 10.1007/s11663-019-01523-1.

[8] A. Plotkowski *et al.*, « Influence of scan pattern and geometry on the microstructure and soft-magnetic performance of additively manufactured Fe-Si », *Additive Manufacturing*, vol. 29, p. 100781, oct. 2019, doi: 10.1016/j.addma.2019.100781.

[9] Q. Liu, Y. Danlos, B. Song, B. Zhang, S. Yin, et H. Liao, « Effect of high-temperature preheating on the selective laser melting of yttria-stabilized zirconia ceramic », *Journal of Materials Processing Technology*, vol. 222, p. 61-74, août 2015, doi: 10.1016/j.jmatprotec.2015.02.036.

[10] R. C. Garvie, R. H. Hannink, et R. T. Pascoe, « Ceramic steel », *Nature (London)*, vol. 258, nº 5537, p. 703-704, déc. 1975.

[11] J. Wilkes, « Selektives Laserschmelzen zur generativen Herstellung von Bauteilen aus hochfester Oxidkeramik », janv. 2009.